NATIONAL ADVISORY COMMITTEE FOR AERONAUTICS

TECHNICAL NOTE

No. 1775

HYDRODYNAMIC IMPACT LOADS IN SMOOTH WATER FOR A PRISMATIC

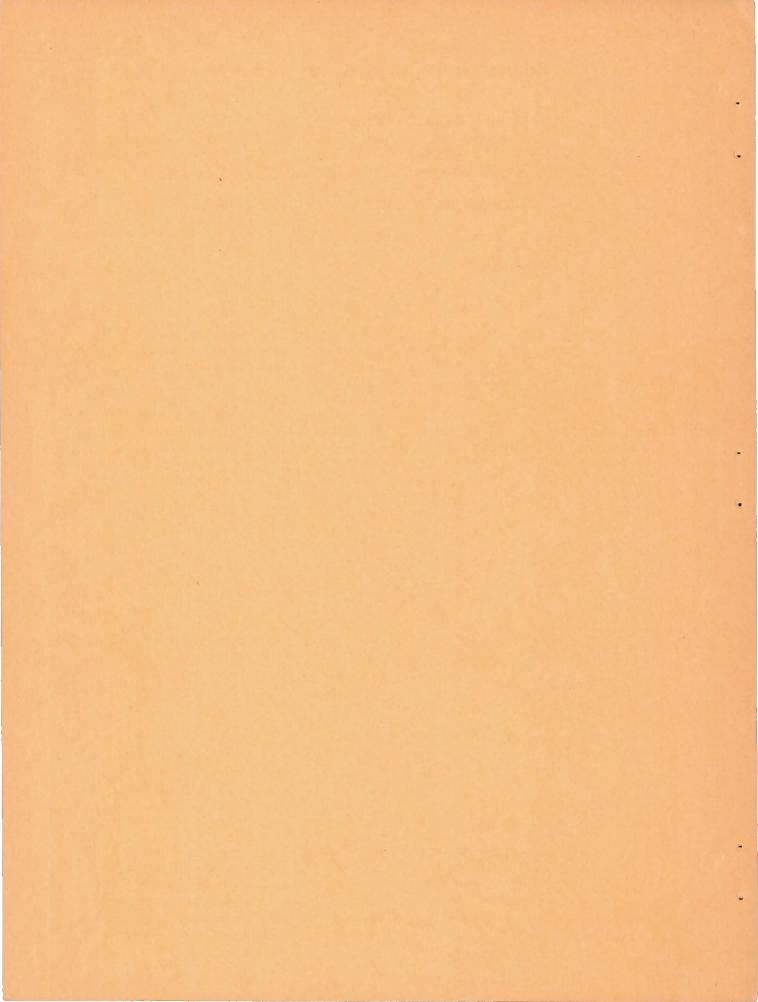FLOAT HAVING AN ANGLE OF DEAD RISE OF 40°

By Philip M. Edge, Jr.

Langley Aeronautical Laboratory
Langley Field, Va.

NACA

Washington

January 1949

HYDRODYNAMIC IMPACT LOADS IN SMOOTH WATER FOR A PRISMATIC

FLOAT HAVING AN ANGLE OF DEAD RISE OF 40°

By Philip M. Edge, Jr.

SUMMARY

A prismatic-float forebody with an angle of dead rise of 40° was subjected to smooth-water impacts in the Langley impact basin. The tests were made at fixed trims of 3°, 6°, 9°, and 12° for a range of flight-path angles from approximately 2° to 22°.

The data are presented and converted into dimensionless variables for correlation of the experimental results with hydrodynamic impact theory and for comparison of the runs among themselves. The average value of the dead-rise function for an angle of dead rise of 40° is evaluated and compared with similar values for angles of dead rise of 30° and $22\frac{1}{2}°$ and with the theoretical dead-rise function. The experimental data are shown to be in good agreement with values predicted by theory.

INTRODUCTION

The development of seaplanes having high aerodynamic performance accompanied by high stalling speeds and high wing loadings has resulted in increased impact loads. The designer of the modern seaplane is confronted with the dual problem of predicting the water loads and of devising means of reducing these loads.

In order to provide a more rational basis for the prediction of impact loads, reference 1 presented an analysis which showed that the motion and time characteristics of an impact may be represented by means of generalized variables. The variation of the generalized variables is governed solely by the magnitude of the approach parameter κ which may be considered a criterion of impact similarity.

One possible means of reducing the water loads on seaplanes is the use of sharper angles of dead rise. A program undertaken at the Langley impact basin to determine the variation of impact loads with angle of dead rise has therefore been expanded to include tests of a seaplane float having a 40° angle of dead rise. Data were obtained at fixed trim with a V-bottom prismatic-float forebody of 40° dead-rise

angle. The data were obtained at the Langley impact basin in smooth
water for a wide range of trim angles, velocities, and flight-path angles.
The test simulated flight conditions in which the effects of the presence
of the afterbody is small. The data are compared with the generalized
theoretical results previously mentioned and the effect of dead-rise
angle on hydrodynamic loads is analyzed.

SYMBOLS

g acceleration due to gravity, 32.2 feet per second^2

n_{i_w} impact load factor, measured normal to water surface, g units

t time after contact, seconds

W dropping weight, pounds

$\dot{x}$ velocity of model parallel to water surface, feet per second

y draft of model normal to water surface, feet

$\dot{y}$ velocity of model normal to water surface, feet per second

β angle of dead rise, degrees

γ flight-path angle relative to water surface, degrees

ρ mass density of water, slugs per cubic foot

τ trim angle, degrees

$f(\beta)$ dead-rise function

$\phi(A)$ aspect-ratio correction factor

Subscripts:

o at water contact

max maximum

Dimensionless variables:

Approach parameter

$$\kappa = \frac{\sin \tau}{\sin \gamma_o} \cos(\tau + \gamma_o)$$

Load-factor coefficient

$$C_l = \frac{n_{i_w} g}{\dot{y}_o^2} \left(\frac{W}{g} \left\{ \frac{6 \sin \tau \cos^2 \tau}{[f(\beta)]^2 \phi(A) \rho \pi} \right\} \right)^{1/3}$$

Draft coefficient

$$C_d = y \left(\frac{g}{W} \left\{ \frac{[f(\beta)]^2 \phi(A) \rho \pi}{6 \sin \tau \cos^2 \tau} \right\} \right)^{1/3}$$

Time coefficient

$$C_t = t \dot{y}_o \left(\frac{g}{W} \left\{ \frac{[f(\beta)]^2 \phi(A) \rho \pi}{6 \sin \tau \cos^2 \tau} \right\} \right)^{1/3}$$

APPARATUS

The Langley impact basin and standard equipment are described in reference 2.

The model tested was the forebody of a prismatic float having a dead-rise angle of $40°$ designated the Langley impact basin model M-3. The model was essentially the same as that used in the tests reported in references 3 and 4, except for the angle of dead rise. The size and shape of the model are defined by the lines and dimensions shown in figure 1. The offsets are given in table I. The model mounted on the carriage boom is shown in figure 2.

The instrumentation used to measure horizontal displacement and velocity and vertical displacement and velocity was described in reference 2. Accelerations in the vertical direction were measured by a standard NACA accelerometer having a natural frequency of 16.5 cycles per second with approximately 0.67 critical damping and a range of -1g to 6g. The contact and exit of the model were determined by means of an electrical circuit completed by the water.

PRECISION

The instrumentation used in the tests gives measurements that are believed accurate within the following limits:

Horizontal velocity, feet per second . . . .   ±0.5
Vertical velocity, feet per second   . . . .   ±0.2
Weight, pounds   . . . .   ±2.0
Acceleration, g . . . .   ±0.35
Time, seconds . . . .   ±0.005
Vertical displacement, inches . . . .   ±0.1

TEST PROCEDURE

The test program was carried out in the Langley impact basin at
fixed trims of 3°, 6°, 9°, and 12° with the float loaded to a weight
of 1213 pounds. A series of impacts in smooth water was made for each of
the four trim angles. The flight-path angle was varied over a range from
approximately 2° to 22° to cover the practical range of flight-path angles
for conventional seaplanes in landing. The range of flight-path angles
was thoroughly covered for the series of tests at 3° and 12° trim whereas
the range of flight-path angles covered at 6° and 9° trim was somewhat
limited. At frequent intervals during the tests, consistency runs were
made with the test conditions as nearly identical as possible. The pur-
pose of these runs was to obtain a check on the consistency of the behavior
of the instrumentation and equipment throughout the investigation. The
data obtained from the consistency runs showed that no significant changes
occurred in the operation and behavior characteristics of the equipment
and instrumentation during the investigation. The data obtained on
these 12 consistency runs were averaged and only the average values are
presented.

The carriage was brought up to testing speed by means of a catapult.
At testing speed the drop linkage was released to permit the model to
acquire vertical velocity under free fall. Once the model had acquired
the proper vertical velocity, a force was produced by a compressed-air
lift engine which counterbalanced the dropping weight of 1213 pounds.
In this manner impacts were made under conditions simulating landings in
which the wing lift is equal to the weight of the seaplane. Subsequent
to the impact the carriage run was terminated by an arresting gear.
This testing procedure is described further in reference 2.

Time histories of horizontal displacement and velocity and of vertical
displacement, velocity, and acceleration were recorded for each run.
Only the vertical component of the impact load is presented as the hori-
zontal component was very small for the trims investigated.

RESULTS AND DISCUSSION

Correlation of Experimental Data with Theoretical Solutions

A theoretical investigation of the motions and hydrodynamic impact loads experienced by V-bottom seaplanes during step-landing impacts is presented in reference 1. The entire immersion process, including the conditions at the instants of maximum acceleration, maximum draft, and rebound, was analyzed from water contact until rebound. This analysis showed that the motion and time characteristics of an impact may be represented by means of generalized variables designated the load-factor coefficient, the draft coefficient, the time coefficient, and the vertical-velocity ratio. The variation of these variables during an impact was shown to be governed solely by the magnitude of the approach parameter κ which depends only on the trim and the flight-path angle at the instant of initial contact with the water and which may be considered a criterion of impact similarity. A single variation with κ consequently exists for each of the generalized variables representing the state of motion and the time corresponding to any given stage of the impact.

The basic data obtained in the present investigation are shown in table I. The experimental data corresponding to the instants of maximum acceleration, maximum draft, and rebound are compared in figures 3 to 6 with the theoretical variations of the generalized variables with the approach parameter, as presented in reference 1. The solid-line curves show the theoretical relationships and the symbols represent the experimental data. Reduction of the experimental data to the form of generalized variables was accomplished by use of the dead-rise

function $f(\beta) = \dfrac{\pi}{2\beta} - 1$ and the aspect-ratio factor $\phi(A) = 1 - \dfrac{\tan \tau}{2 \tan \beta}$.
These relations were presented in reference 5 and correspond to the theoretical and experimental relations obtained by reference 6 and reference 7, respectively.

The variation of load-factor coefficient

$$C_l = \frac{n_{i_w}g}{\dot{y}_o^2} \left(\frac{W}{g} \left\{ \frac{6 \sin \tau \cos^2 \tau}{[f(\beta)]^2 \phi(A) \rho \pi} \right\} \right)^{1/3} \tag{1}$$

with approach parameter κ is shown in figure 3. The upper curve shows the maximum load-factor coefficient, whereas the lower curve shows the load-factor coefficient at the instant of maximum draft. The experimental values agree well with the theoretical variation of maximum load-factor coefficient with approach parameter. At the time of maximum draft, however, the experimental values show greater scatter as a result of the inaccuracies in measuring the time of maximum draft and the acceleration at that time.

At high values of κ the trend of the experimental variation at
maximum draft is below the theoretical curve and indicates somewhat
lower accelerations. These low values of acceleration are believed to
result from the time lag in the displacement measurements which results
in recorded values of the time of maximum draft that are slightly greater
than the actual time of maximum draft. Since the time of maximum draft
occurs after the time of maximum acceleration, the greater the time lag
of maximum draft, the smaller the acceleration at the indicated time of
maximum draft. At low values of κ (high flight-path angles) the trend
of the experimental data at maximum draft is somewhat above the theoretical
curve. This result is explained by the presence of buoyant forces, which
were neglected in the theoretical solutions. These buoyant forces become
of significance only at high flight-path angles beyond the range for
conventional seaplanes.

The variation of draft coefficient

$$C_d = y \left(\frac{g}{W} \left\{ \frac{[f(\beta)]^2 \phi(A) \rho \pi}{6 \sin \tau \cos^2 \tau} \right\} \right)^{1/3} \tag{2}$$

with approach parameter κ is presented in figure 4. The upper curve
shows the maximum draft coefficient and the lower curve shows the draft
coefficient at time of maximum acceleration. The experimental data are
in good agreement with the theoretical curves.

The variation of time coefficient

$$C_t = t\dot{y}_0 \left(\frac{g}{W} \left\{ \frac{[f(\beta)]^2 \phi(A) \rho \pi}{6 \sin \tau \cos^2 \tau} \right\} \right)^{1/3} \tag{3}$$

with the approach parameter κ is shown in figure 5. The upper curve
shows values for the time coefficient at the instant that the model
leaves the water on the rebound. The middle curve shows the time coeffi-
cient at the instant of maximum draft. The lower curve shows the time
coefficient at the instant of maximum acceleration. The test points
show good agreement with the theoretical curves; the buoyant forces
again account for the lower values of the experimental data at low values
of κ (high flight-path angles).

In figure 6, the ratio of vertical velocity to initial vertical
velocity $\dot{y}/\dot{y}_0$ is plotted against the approach parameter κ. The
upper curve shows this ratio at the instant of maximum acceleration and
the lower curve shows the ratio at the instant of rebound. The experi-
mental data show general agreement with the theoretical curves despite
the low measured values of velocity which result in greater scatter of
the points because of measurement error.

The discrepancy between the theoretical and experimental values of the vertical-velocity ratio at the instant of rebound is attributed to friction and leakage in the compressed-air lift mechanism which balanced the weight. The leakage takes effect after the maximum draft has been reached and has a maximum effect on the motion at the instant of rebound. In addition, greater scatter is present at this instant because of the variation in the time lag of the instrumentation which was used to measure vertical velocity.

In some cases the model was immersed beyond the limits of the prismatic shape (72 inches long by 17.25 inches high - see fig. 1). The general agreement of the data with the theory, however, indicates that the effects of bow and chine immersion were of no great significance.

Effect of Dead-Rise Angle on Hydrodynamic Load

From the form of the load-factor coefficient it can be seen that, if all other parameters are held constant, the hydrodynamic load is proportional to the quantity $[f(\beta)]^{2/3}$ where $f(\beta) = \frac{\pi}{2\beta}-1$. If the conventional dead-rise angle of $22\frac{1}{2}^\circ$ is used as a base, this relationship indicates a reduction in load of 24 percent for an angle of dead rise of 30° and a reduction of 44 percent for an angle of dead rise of 40°

The validity of the theoretical variation of hydrodynamic load with dead rise was verified for angles of dead rise of $22\frac{1}{2}^\circ$ and 30° by experimental data obtained in the Langley impact basin (references 1, 3, and 4). In the present paper, the range of dead-rise angle is extended to 40°. The data previously presented in figure 3 are further analyzed to determine an experimental value of the dead-rise function $[f(\beta)]^{2/3}$.

Solving equation (1) for $[f(\beta)]^{2/3}$ gives

$$[f(\beta)]^{2/3} = \frac{n_{i_w}g}{C_l \dot{y}_o^2} \left\{ \frac{W}{g} \left[\frac{6 \sin \tau \cos^2 \tau}{\phi(A)\pi\rho} \right] \right\}^{1/3} \tag{4}$$

From the theoretical relationship between $C_{l_{max}}$ and κ of reference 1, a theoretical value of $C_{l_{max}}$ is obtained corresponding to the approach parameter κ computed for each run (table II). Substituting this value of C_l and the data of table II into equation (4) gives an experimental value of $[f(\beta)]^{2/3}$ for each run. The distribution or resulting experimental values of $[f(\beta)]^{2/3}$ is shown in figure 7, where the distributions are grouped as percentages of the total number of values used. This figure shows that the distribution about the average value is approximately normal and indicates that the deviation from the normal is largely random.

Figure 8 shows the variation of the dead-rise function with the angle of dead rise. Since the dead-rise function is plotted as $[f(\beta)]^{2/3}$ this curve also shows the variation of hydrodynamic load with angle of dead rise. The solid-line curve shows the theoretical variation given by $[f(\beta)]^{2/3} = \left(\frac{\pi}{2\beta} - 1\right)^{2/3}$. The symbols represent experimental values of the dead-rise variation determined by averaging each group of data obtained with floats of $40°$, $30°$, and $22\frac{1}{2}°$ angles of dead rise, respectively. The value shown for a dead-rise angle of $40°$ is the average corresponding to the distribution shown in figure 7. The average values for angles of dead rise of $30°$ and $22\frac{1}{2}°$ were obtained in a similar manner and were presented in reference 4. Figure 8 shows that the hydrodynamic load decreases appreciably (44 percent) as the angle of dead rise is increased from $22\frac{1}{2}°$ to $40°$. The variation of the average values of the experimental data agrees well with the theoretical variation.

CONCLUSIONS

An analysis of experimental data obtained by subjecting a prismatic float having an angle of dead rise of $40°$ to impacts in smooth water results in the following conclusions:

1. Experimental values of the load-factor coefficient, draft coefficient, time coefficient, and vertical-velocity ratio corresponding to the instants of maximum acceleration, maximum draft, and rebound are in good agreement with values predicted by hydrodynamic impact theory.

2. If all other parameters are held constant, the hydrodynamic load for a seaplane having an angle of dead rise of $40°$ is 44 percent less than the hydrodynamic load for the seaplane with a conventional dead-rise angle of $22\frac{1}{2}°$.

Langley Aeronautical Laboratory
    National Advisory Committee for Aeronautics
        Langley Field, Va., September 28, 1948

REFERENCES

1. Milwitzky, Benjamin: A Generalized Theoretical and Experimental
   Investigation of the Motions and Hydrodynamic Loads Experienced by
   V-Bottom Seaplanes During Step-Landing Impacts. NACA TN
   No. 1516, 1948.

2. Batterson, Sidney A.: The NACA Impact Basin and Water Landing Tests
   of a Float Model at Various Velocities and Weights. NACA Rep.
   No. 795, 1944.

3. Mayo, Wilbur L.: Theoretical and Experimental Dynamic Loads for a
   Prismatic Float Having an Angle of Dead Rise of $22\frac{1}{2}^\circ$. NACA RB
   No. L5F15, 1945.

4. Miller, Robert W., and Leshnover, Samuel: Hydrodynamic Impact Loads
   in Smooth Water for a Prismatic Float Having an Angle of Dead Rise
   of 30°. NACA TN No. 1325, 1947.

5. Mayo, Wilbur L.: Analysis and Modification of Theory for Impact of
   Seaplanes on Water. NACA Rep. No. 810, 1945.

6. Wagner, Herbert: Über Stoss- und Gleitvorgänge an der Oberfläche
   von Flüssigkeiten. Z.f.a.M.M., Bd. 12, Heft 4, Aug. 1932,
   pp. 193-215.

7. Pabst, Wilhelm: Theory of the Landing Impact of Seaplanes. NACA TM
   No. 580, 1930.

TABLE I . - OFFSETS OF LANGLEY IMPACT-BASIN

FLOAT MODEL M-3 (SEE FIG. 1)

[All dimensions are in inches]

Station	Half breadth		Height above datum line		
	Chine	Deck	Keel	Chine	Deck
0	0	0.33	27.06	27.06	37.60
2	2.15	1.45	21.34	26.08	38.17
5	4.25	3.05	17.12	25.97	38.81
9	7.80	4.58	12.85	27.06	39.51
14	10.31	5.93	9.05	24.90	40.09
21	12.81	7.23	5.62	21.90	40.52
29	15.09	8.15	3.01	19.08	40.59
38	16.86	8.71	1.13	16.55	40.59
47	18.04	8.94	.27	15.53	40.59
58	18.87	9.00	0	15.56	40.59
72	19.33	9.00	0	15.94	40.59
87.25	19.40	9.00	0	16.00	40.59
106.625	19.40	9.00	0	16.00	40.59
120.75	19.40	9.00	0	16.00	40.59

NACA

TABLE II

IMPACT-LOADS DATA FROM TESTS OF A PRISMATIC FLOAT

WITH 40° ANGLE OF DEAD RISE

Run	At contact			Approach parameter, κ	At $n_{1_{w max}}$				Time, t, at chine immersion (sec)	Time, t, at bow immersion (sec)	At y_{max}			At rebound	
	$\dot{y}_0$ (fps)	$\dot{x}_0$ (fps)	γ_0 (deg)		t (sec)	n_{1_w} (g)	y (ft)	$\dot{y}$ (fps)			t (sec)	y (ft)	n_{1_w} (g)	t (sec)	$\dot{y}$ (fps)
								$\tau = 3°$							
1	9.24	23.31	21.62	0.129	0.082	1.60	0.68	7.32	0.285	0.035	0.377	1.49	0.32	-------	-------
2	7.75	23.26	18.43	.154	.103	1.17	.74	5.97	None	.040	.396	1.39	.25	-------	-------
3	9.39	29.82	17.48	.163	.088	1.76	.78	7.04	.315	.033	.344	1.46	.32	No exit	No exit
4	8.82	29.07	16.88	.170	.077	1.70	.69	7.39	.337	.035	.356	1.45	.25	--do---	Do.
5	7.61	28.74	14.83	.195	.100	1.26	.71	5.69	None	.038	.370	1.33	.15	--do---	Do.
6	7.82	29.94	14.64	.197	.093	1.30	.72	5.90	-do-	.038	.360	1.30	.32		Do.
7	9.39	40.32	13.11	.222	.098	1.99	.83	6.26	-do-	.038	.309	1.29	.28	--do---	Do.
8	8.75	39.53	12.48	.233	.087	1.82	.73	6.47	-do-	.035	.312	1.30	.25	--do---	Do.
9	7.89	40.32	11.07	.264	.094	1.48	.68	6.19	-do-	.041	.322	1.20	.32	--do---	Do.
10	4.05	23.15	9.92	.296	.180	.41	.66	2.70	-do-	.142	.455	.96	.20	--do---	Do.
11	9.46	56.50	9.51	.309	.082	2.17	.72	6.90	-do-	.032	.247	1.16	.32	1.067	-0.57
12	5.83	40.32	8.23	.359	.128	.87	.63	4.05	-do-	.058	.353	1.00	.25	No exit	No exit
13	8.11	56.50	8.17	.361	.102	1.70	.75	5.55	-do-	.042	.266	1.08	.36	--do---	Do.
14	7.47	54.35	7.83	.377	.098	1.52	.67	5.26	-do-	.040	.268	1.04	.28	--do---	Do.
15	9.39	69.93	7.65	.386	.080	2.37	.69	6.97	-do-	.030	.232	1.06	.38	.871	-.85
16	3.13	23.36	7.63	.387	.213	.25	.57	1.99	-do-	.104	.488	.85	.08	No exit	No exit
17	4.05	30.30	7.61	.389	.162	.45	.58	2.99	-do-	.084	.420	.94	.19	--do---	Do.
18	8.03	68.49	6.69	.443	.097	1.76	.69	5.33	-do-	.036	.242	.97	.38	--do---	Do.
19	5.97	56.50	6.03	.492	.117	1.05	.64	4.12	-do-	.052	.286	.89	.32	--do---	Do.
20	2.84	27.32	5.93	.501	.252	.27	.62	1.49	-do-	.110	.473	.77	.08	--do---	Do.
21	3.13	30.30	5.90	.503	.213	.27	.58	1.99	-do-	.102	.428	.77	.15	--do---	Do.
22	4.05	39.37	5.87	.506	.165	.50	.59	2.70	-do-	.076	.360	.81	.28	--do---	Do.
23	3.98	40.16	5.66	.525	.161	.50	.58	2.70	-do-	.076	.366	.83	.15	--do---	Do.
24	3.84	39.21	5.59	.531	.170	.45	.56	2.49	-do-	.086	.401	.79	.10	--do---	Do.
25	7.82	91.50	5.11	.582	.084	2.03	.59	5.69	-do-	.031	.197	.86	.63	.612	-1.71
26	5.69	68.49	4.75	.626	.120	1.14	.59	3.77	-do-	.053	.260	.79	.32	No exit	No exit
27	2.84	39.06	4.16	.716	.248	.30	.58	1.28	-do-	.116	.408	.68	.08	--do---	Do.
28	3.77	54.64	3.95	.754	.163	.57	.59	2.20	-do-	.073	.321	.73	.15	--do---	Do.
29	5.69	90.10	3.61	.826	.111	1.26	.58	3.56	-do-	.054	.228	.73	.50	--do---	Do.
30	4.27	68.03	3.59	.830	.148	.72	.55	2.70	-do-	.074	.278	.69	.31	--do---	Do.
31	3.20	56.18	3.26	.915	.183	.41	.52	1.85	-do-	.092	.350	.66	.20	--do---	Do.
32	3.56	68.03	3.00	.995	.184	.57	.56	1.78	-do-	.087	.284	.63	.40	--do---	Do.
33	3.20	68.49	2.68	1.114	.185	.50	.53	1.78	-do-	.107	.314	.61	.15	--do---	Do.
34	4.12	90.10	2.62	1.140	.141	.84	.51	2.42	-do-	.069	.241	.63	.45	.710	-0.57
35	3.63	90.09	2.31	1.293	.154	.75	.50	1.85	-do-	.088	.247	.58	.35	No exit	No exit
36	2.77	90.91	1.75	1.708	.193	.49	.44	1.14	-do-	.078	.277	.48	.15	--do---	Do.
(a)	9.02	89.88	5.73	.520	.083	2.59	.67	5.90	-do-	.037	.192	.95	.72	.756	-1.70
								$\tau = 6°$							
37	8.89	34.13	14.60	0.388	0.107	1.72	0.89	6.26	-do-	0.072	0.296	1.35	0.32	1.085	-1.07
38	8.75	34.60	14.19	.400	.108	1.85	.91	5.90	-do-	.068	.293	1.33	.32	1.044	-1.28
39	8.89	35.21	14.17	.401	.094	1.76	.81	6.33	-do-	.068	.284	1.30	.36	.975	-1.35
40	9.03	43.47	11.74	.489	.100	1.98	.85	6.33	-do-	.067	.253	1.22	.50	.836	-2.28
41	8.89	43.29	11.61	.495	.102	1.99	.85	6.04	-do-	.071	.253	1.22	.45	.849	-1.71
42	8.75	44.25	11.19	.515	.107	1.98	.85	6.11	-do-	.062	.252	1.18	.50	.839	-1.71
43	8.89	46.73	10.77	.536	.094	2.03	.81	6.47	-do-	.069	.234	1.18	.58	.772	-1.99
44	8.89	58.14	8.69	.669	.100	2.29	.81	5.90	-do-	.071	.209	1.08	.75	.602	-2.56
45	8.96	58.47	8.46	.688	.100	2.33	.81	5.76	-do-	.063	.209	1.07	.80	.612	-2.42
46	8.96	60.97	8.36	.697	.101	2.29	.82	5.83	-do-	.067	.206	1.10	.89	.615	-2.35
47	9.03	66.22	7.77	.751	.090	2.45	.74	5.76	-do-	.075	.195	1.01	1.00	.557	-2.70
48	8.75	65.36	7.63	.765	.094	2.37	.76	5.83	-do-	.071	.194	1.02	.83	.557	-2.77
49	8.67	85.47	5.79	1.014	.091	2.75	.74	5.12	-do-	.071	.116	.89	1.13	.432	-3.34
50	8.53	86.21	5.65	1.040	.090	2.80	.70	5.26	-do-	.076	.170	.86	1.32	.421	-3.34
51	2.99	43.48	3.93	1.502	----	.40	---	1.35	----	----	----	----	----	----	-----
52	2.99	43.67	3.92	1.506	.210	.40	.42	1.35	none	.286	.349	.63	.25	----	-----
53	2.77	43.10	3.68	1.605	.238	.36	.56	1.21	-do-	.333	.352	.63	.20	No exit	No exit

[a]Average of consistency runs.

NACA

TABLE II - Concluded

IMPACT-LOADS DATA FROM TESTS OF A PRISMATIC FLOAT

WITH 40° ANGLE OF DEAD RISE - Concluded

Run	At contact			Approach parameter, κ	At $n_{i_{w_{max}}}$				Time, t, at chine immersion (sec)	Time, t, at bow immersion (sec)	At y_{max}			At rebound	
	$\dot{y}_0$ (fps)	$\dot{x}_0$ (fps)	γ_0 (deg)		t (sec)	n_{i_w} (g)	y (ft)	$\dot{y}$ (fps)			t (sec)	y (ft)	n_{i_w} (g)	t (sec)	$\dot{y}$ (fps)
τ = 9°															
54	9.24	35.59	14.55	0.571	0.115	1.85	0.96	5.76	None	None	0.258	1.29	0.58	0.825	-2.13
55	9.24	44.44	11.75	.718	.103	2.16	.87	6.33	-do-	.108	.230	1.18	.75	.648	-2.63
56	9.46	45.45	11.76	.718	.100	2.25	.87	6.75	-do-	.110	.230	1.19	.88	.655	-2.63
57	9.53	45.87	11.74	.719	.102	2.29	.93	8.03	-do-	.107	.212	1.22	.92	.642	-2.77
58	9.46	46.08	11.60	.728	.104	2.25	.88	6.61	-do-	.114	.226	1.21	.80	.654	-2.77
59	8.96	51.55	9.86	.864	.104	2.28	.85	5.76	-do-	.074	.207	1.09	1.08	.565	-3.06
60	9.10	58.82	8.79	.975	.102	2.55	.84	5.47	-do-	.117	.176	1.04	1.25	.494	-3.56
61	8.60	57.14	8.56	1.002	.104	2.37	.81	5.33	-do-	.082	.194	1.03	1.18	.522	-3.13
62	8.75	63.69	7.82	1.101	.106	2.55	.82	5.05	-do-	.128	.181	.98	1.30	.466	-3.70
63	8.89	65.79	7.70	1.118	.099	2.71	.82	5.40	-do-	.124	.175	.99	1.52	.450	-3.84
64	9.03	77.51	6.65	1.301	.101	2.97	.77	5.12	-do-	None	.151	.91	1.52	.391	-4.05
65	8.60	76.34	6.43	1.347	.109	2.67	.80	4.19	-do-	-do-	.167	.90	1.57	.405	-3.98
66	8.67	86.20	5.74	1.513	----	3.27	---	3.98	-do-	-do-	----	----	2.00	.343	-4.48
67	8.60	86.96	5.65	1.537	.105	2.97	.76	4.12	-do-	-do-	.155	.84	1.57	.365	-4.34
68	3.27	43.48	4.30	2.030	.227	.50	.62	1.35	-do-	-do-	.317	.68	.28	.938	-.50
69	3.12	44.64	4.00	2.185	.218	.45	.54	1.49	-do-	-do-	.318	.61	.25	.902	-.64
70	2.98	58.48	2.92	3.005	.210	.55	.51	1.14	-do-	-do-	.272	.54	.35	.663	-1.35
71	2.92	60.34	2.78	3.157	.212	.55	.50	1.07	-do-	-do-	.280	.54	.32	.662	-1.28
τ = 12°															
72	9.46	23.15	22.23	0.454	0.130	1.65	1.14	6.26	0.201	0.145	0.339	1.63	0.41	1.202	-0.92
73	7.96	23.04	19.06	.545	.129	1.23	.95	5.83	.257	.174	.344	1.47	.35	1.145	-1.42
74	9.53	29.67	17.81	.590	.130	1.86	1.09	5.83	.202	.146	.270	1.47	.63	.905	-1.85
75	9.10	30.03	16.86	.628	.117	1.73	1.02	6.19	.153	.149	.278	1.43	.50	.870	-2.13
76	8.11	30.12	15.07	.712	.130	1.47	.92	5.62	None	.207	.280	1.29	.50	.897	-1.78
77	9.46	39.84	13.36	.813	.115	2.17	.99	6.04	-do-	.192	.217	1.28	.85	.642	-2.92
78	9.24	39.84	13.06	.834	.115	2.16	.93	5.76	-do-	None	.225	1.20	.96	.628	-3.06
79	7.75	39.53	11.09	.994	.140	1.65	.94	4.34	-do-	-do-	.240	1.12	.80	.650	-2.77
80	7.96	40.98	10.99	1.004	.139	1.73	.94	4.48	-do-	-do-	.229	1.12	.87	.632	-2.99
81	4.05	22.83	10.06	1.103	.247	.45	.85	2.06	-do-	-do-	.413	.98	.15	----	-----
82	9.39	56.18	9.49	1.173	.120	2.64	.95	4.19	-do-	-do-	.183	1.08	----	No exit	No exit
83	8.11	56.18	8.21	1.365	.126	2.17	.71	3.98	-do-	-do-	.189	.83	1.52	.467	-3.91
84	5.83	40.65	8.16	1.376	.157	1.14	.80	3.34	-do-	-do-	.256	.95	.60	.684	-2.28
85	4.34	30.40	8.12	1.382	.235	.66	.81	1.85	-do-	-do-	.350	.90	.36	1.001	-.71
86	9.53	69.44	7.81	1.439	.105	3.24	.86	4.76	-do-	-do-	.155	.97	2.05	.372	-4.98
87	9.03	68.03	7.56	1.489	.105	2.97	.81	4.91	-do-	-do-	.160	.93	1.25	.378	-4.62
88	7.75	68.49	6.46	1.753	.118	2.33	.76	3.91	-do-	-do-	.170	.85	1.43	.402	-4.12
89	7.61	68.49	6.34	1.787	.121	2.32	.78	3.41	-do-	-do-	.171	.85	1.48	.391	-4.12
90	4.34	40.98	6.05	1.876	.194	.75	.70	2.06	-do-	-do-	.288	.79	.58	.730	-1.56
91	3.06	29.33	5.96	1.905	.260	.40	.71	1.49	-do-	-do-	.392	.77	.20	No exit	No exit
92	9.24	90.09	5.86	1.938	.104	3.68	.76	4.27	-do-	-do-	.137	.81	2.98	.304	-5.40
93	5.76	56.50	5.82	1.952	.150	1.38	.72	2.77	-do-	-do-	.210	.81	.96	.504	-2.99
94	9.10	89.29	5.82	1.952	.099	3.57	.73	4.41	-do-	-do-	.139	.81	3.10	.304	-5.33
95	3.98	39.37	5.77	1.969	.200	.65	.67	1.85	-do-	-do-	.299	.78	.40	.750	-1.64
96	8.75	91.00	5.49	2.073	.104	3.57	.76	3.56	-do-	-do-	.134	.80	2.37	.299	-5.19
97	7.68	90.91	4.83	2.364	.115	2.97	.70	2.99	-do-	-do-	.151	.75	2.25	.315	-4.55
98	7.54	89.29	4.83	2.364	.107	2.92	.63	3.27	-do-	-do-	.141	.68	2.15	.310	-4.62
99	5.69	68.49	4.75	2.404	.155	1.56	.67	2.20	-do-	-do-	.189	.69	1.35	.426	-3.06
100	3.27	40.49	4.62	2.473	.238	.50	.59	1.35	-do-	-do-	.319	.65	.32	.871	-.57
101	5.33	68.03	4.48	2.552	.144	1.52	.65	2.13	-do-	-do-	.198	.70	1.00	.433	-3.13
102	4.12	55.87	4.22	2.713	.190	.87	.62	1.35	-do-	-do-	.250	.64	.63	.565	-2.13
103	4.27	68.03	3.59	3.198	.178	1.05	.54	1.21	-do-	-do-	.220	.55	.70	.477	-2.42
104	4.98	90.09	3.16	3.640	.125	1.76	.55	2.28	-do-	-do-	.160	.58	1.48	.350	-3.48
105	3.20	67.57	2.71	4.253	.208	.66	.51	1.14	-do-	-do-	.278	.53	.50	.628	-1.35
106	2.92	68.49	2.44	4.729	.212	.66	.46	.57	-do-	-do-	.242	.47	.55	.552	-1.49
107	3.70	90.09	2.35	4.913	.146	1.13	.45	1.35	-do-	-do-	.186	.48	.96	.389	-2.49
108	3.13	90.09	1.99	4.810	.180	.92	.42	.43	-do-	-do-	.205	.42	.80	.410	-1.99

NACA

Deck

Chine

0 2 5 9 14 21 29 38 47 58 72 87.25 106.62.5 120.75

19.4"

9.0"

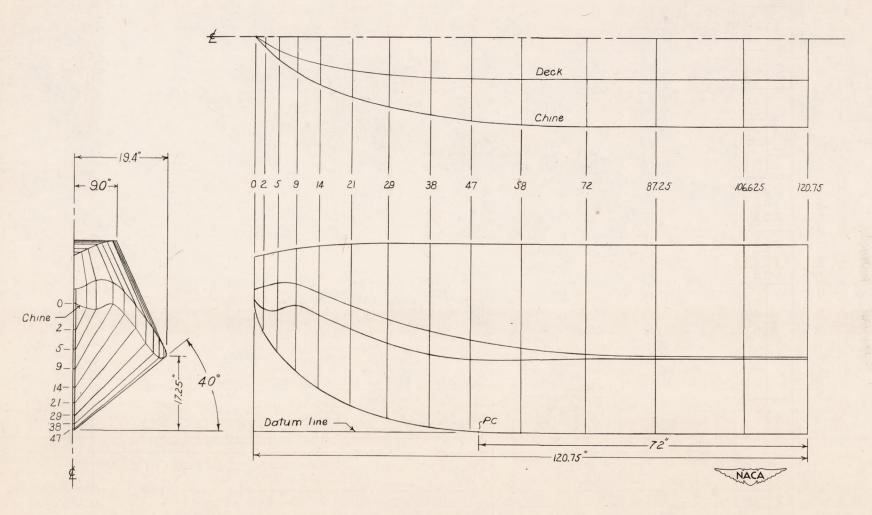Chine

0
2
5
9
14
21
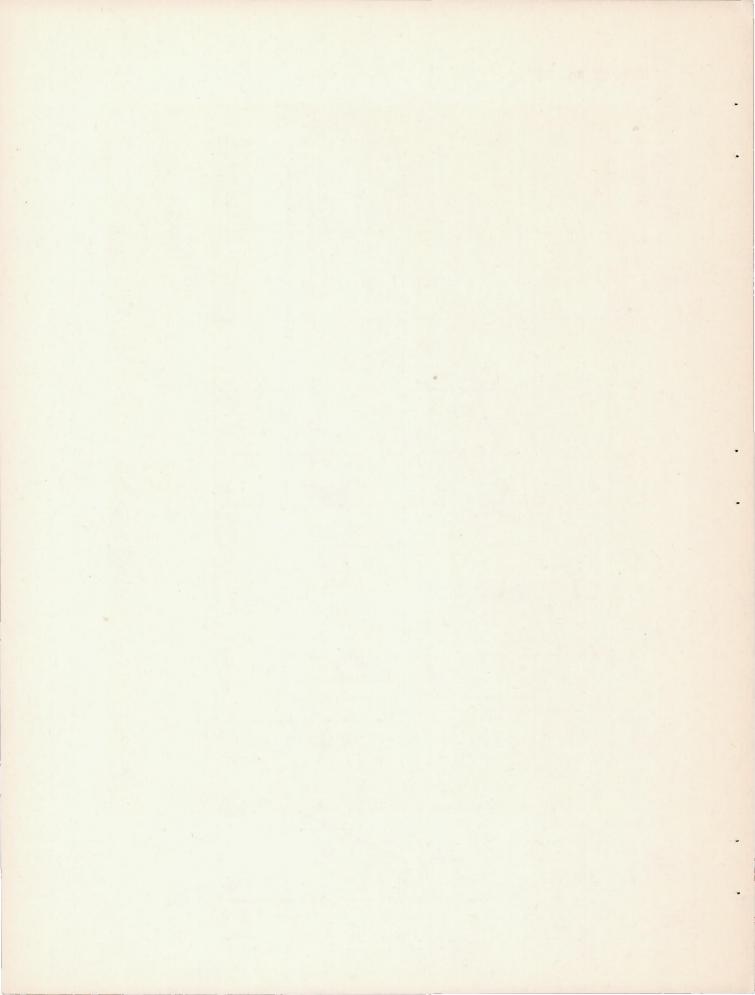29
38
47

17.25"

40°

Datum line

PC

72"

120.75"

NACA

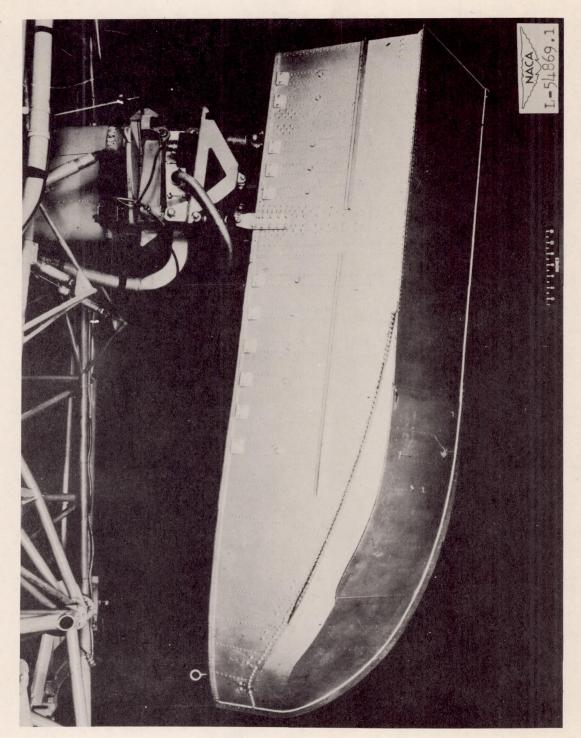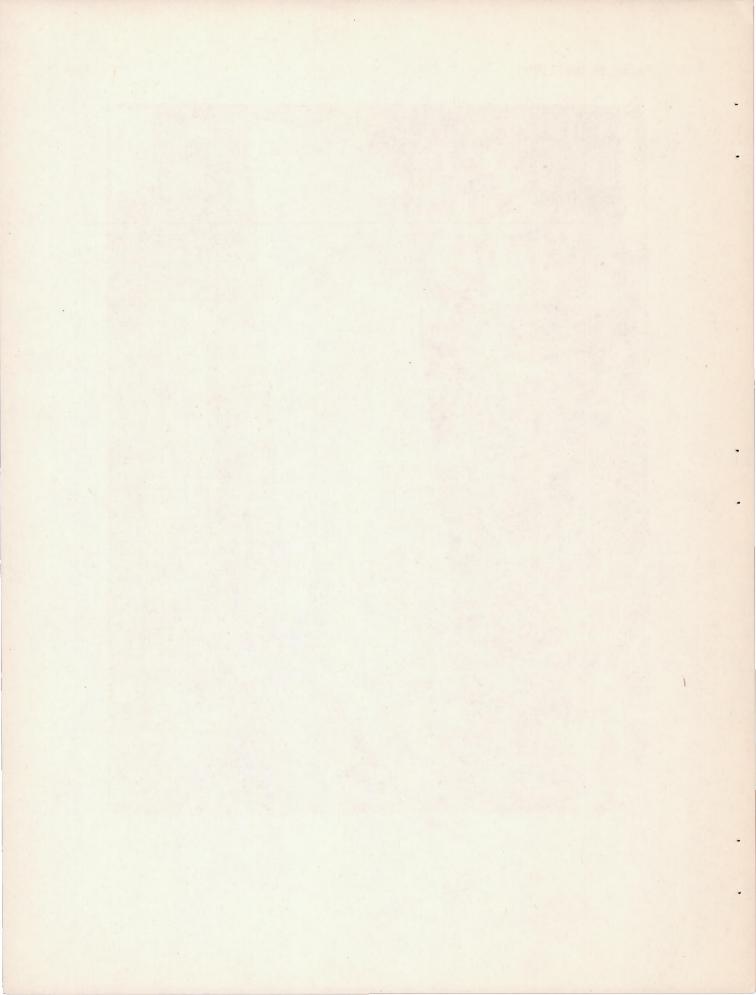Figure 1.- Lines of Langley impact-basin float model M-3.

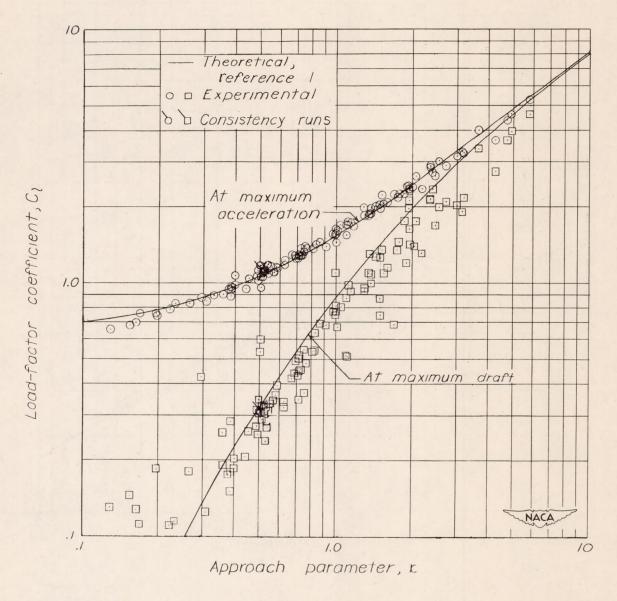Figure 2.- Langley impact-basin float model M-3.

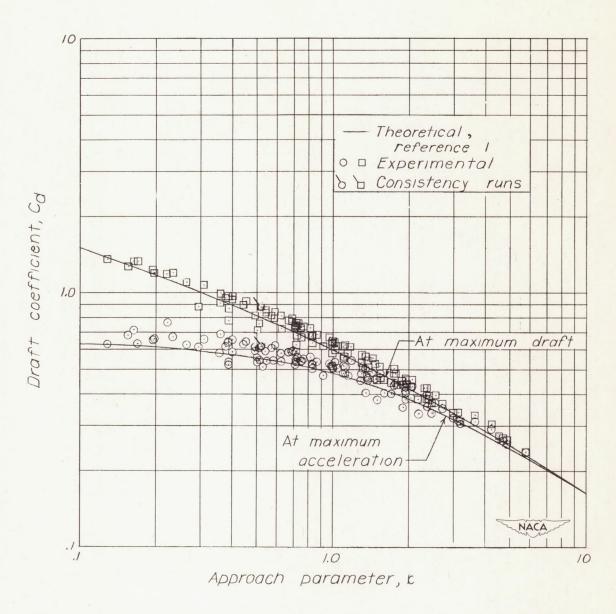Figure 3.—Variation of load-factor coefficient with approach parameter.

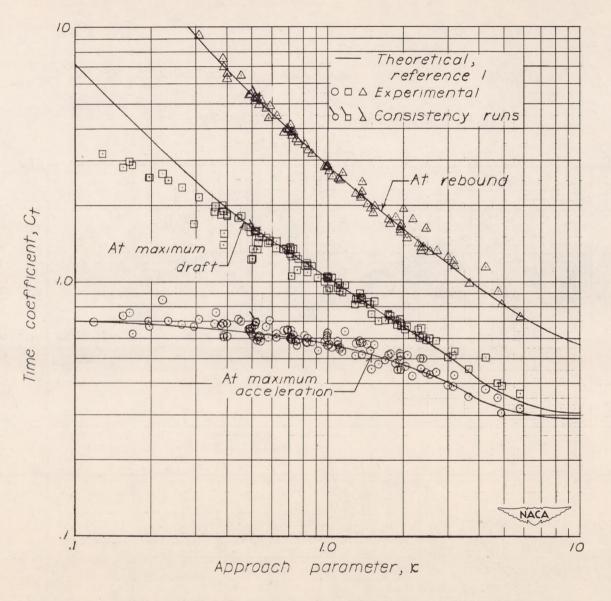Figure 4.-Variation of draft coefficient with approach
parameter.

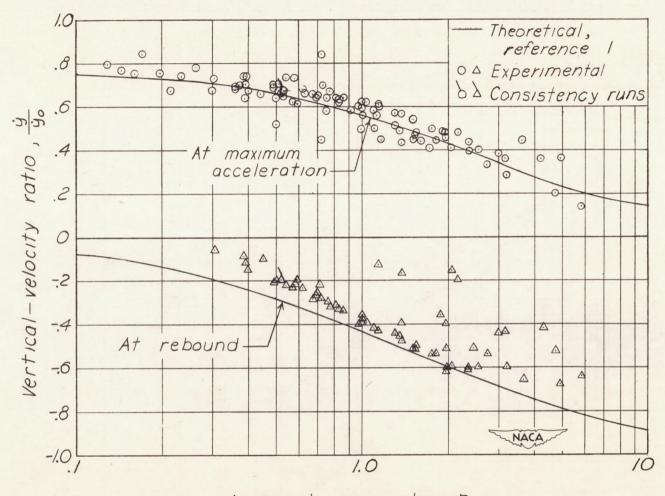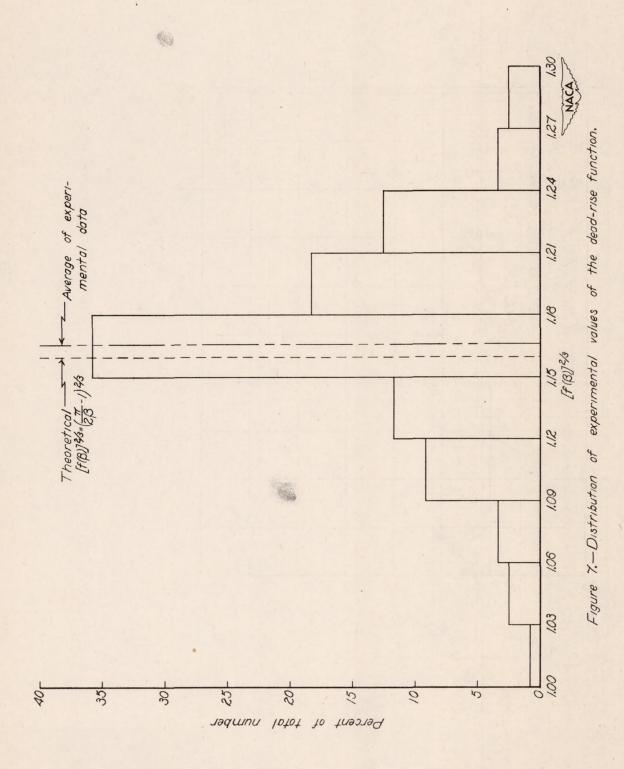Figure 5.—Variation of time coefficient with approach parameter.

Figure 6.- Variation of vertical velocity with approach parameter.

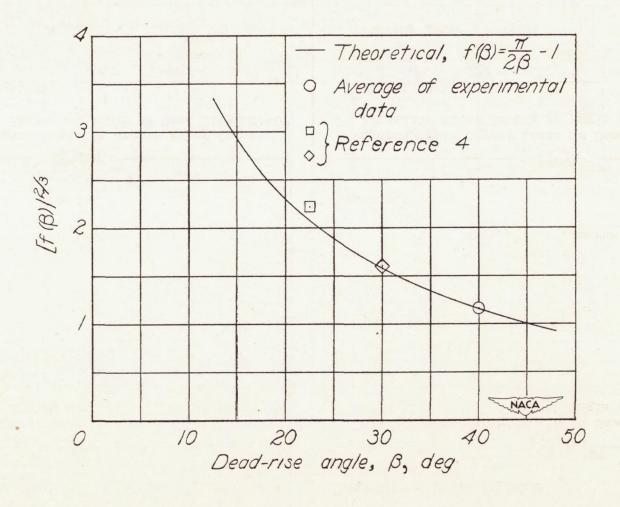Figure 7.—Distribution of experimental values of the dead-rise function.

Figure 8.— Theoretical and experimental values of
dead-rise function.